EBioMedicine 6 (2016) 139–148

Contents lists available at ScienceDirect

EBioMedicine

journal homepage: www.ebiomedicine.com

Research Paper

Irisin Inhibits Hepatic Cholesterol Synthesis via AMPK-SREBP2 Signaling

Hong Tang [a], Ruili Yu [a], Shiying Liu [a], Bahetiyaer Huwatibieke [a], Ziru Li [b], Weizhen Zhang [a,b,*]

[a] Department of Physiology and Pathophysiology, Peking University Health Science Center, Beijing 100191, China
[b] Department of Surgery, University of Michigan Medical Center, Ann Arbor, MI 48109-0346, USA

ARTICLE INFO

Article history:
Received 5 November 2015
Received in revised form 23 February 2016
Accepted 25 February 2016
Available online 27 February 2016

Keywords:
Irisin
AMPK
SREBP2
Cholesterol
Liver

ABSTRACT

Irisin, a myokine released during exercise, promotes browning of subcutaneous adipose tissue and regulates energy homeostasis. Although exercise constantly reduces blood cholesterol, whether irisin is involved in the regulation of cholesterol remains largely unknown. In the present study, subcutaneous infusion of irisin for 2 weeks induced a reduction in plasma and hepatic cholesterol in high fat diet-induced obese (DIO) mice. These alterations were associated with an activation of 5′ AMP-activated protein kinase (AMPK) and inhibition of sterol regulatory element-binding transcription factor 2 (SREBP2) transcription and nuclear translocation. In primary hepatocytes from either lean or DIO mice, irisin significantly decreased cholesterol content via sequential activation of AMPK and inhibition of SREBP2. Suppression of AMPK by compound C or AMPKα1 siRNA blocked irisin-induced alterations in cholesterol contents and SREBP2. In conclusion, irisin could suppress hepatic cholesterol production via a mechanism dependent of AMPK and SREBP2 signaling. These findings suggest that irisin is a promising therapeutic target for treatment of hypercholesterolemia.

1. Introduction

Irisin was recently identified as a myokine proteolytically cleaved from fibronectin type β domain containing 5 (FNDC5) (Bostrom et al., 2012). Exercise could induce irisin expression and secretion into circulation to exert its effects on browning of subcutaneous adipose tissue (Bostrom et al., 2012; Wu et al., 2014; Shan et al., 2013; Rodriguez et al., 2015; Lee et al., 2014; Wu et al., 2012), as well as subsequent improvement of obesity (Huh et al., 2014; Miyamoto-Mikami et al., 2015) and its related disorders such as type 2 diabetes (Xiong et al., 2015; Bostrom et al., 2012; Vaughan et al., 2014). These observations suggest that irisin may contribute to the regulation of energy homeostasis and thus is the potential target for therapy of metabolic dysfunction associated with obesity. This concept is further supported by clinical observations. Circulating irisin was found to be reduced in obese human (Yan et al., 2014; Moreno-Navarrete et al., 2013; Duran et al., 2015; Hou et al., 2015) and rodents (Bilski et al., 2015) and in patients with diabetes (Espes et al., 2015; Li et al., 2015a; Choi et al., 2013; Xiang et al., 2014; Liu et al., 2013; Duran et al., 2015; Moreno-Navarrete et al., 2013; Kurdiova et al., 2014), or chronic kidney disease (Wen et al., 2013; Ebert et al., 2014). Conversely, it was positively associated with endothelium-dependent vasodialation (Xiang et al., 2014; Hou et al., 2015; Zhu et al., 2015) and myocardiac infraction in type 2 diabetes (Aronis et al., 2015; Hou et al., 2015).

The relationship between irisin and lipid metabolism has been controversial. Evidence suggesting a negative relation between irisin and lipid dysregulation has been emerging. Circulating levels of irisin were negatively correlated with total cholesterol, LDL cholesterol and triglyceride (Huh et al., 2012; Zhang et al., 2013; Ebert et al., 2015; Duran et al., 2015) and intrahepatic triglyceride contents in obese adults (Zhang et al., 2013), while positively correlated with HDL cholesterol. In obese human, diet intervention-induced reduction in glucose and triglyceride was greater in those with higher baseline irisin levels (Lopez-Legarrea et al., 2014). Lentivirus-mediated overexpression of FNDC5 or subcutaneous perfusion of irisin reduced blood triglyceride, cholesterol, free fatty acid and glucose in obese mice (Xiong et al., 2015). Further studies in vitro showed an inhibitory effect of irisin on palmitic acid (PA)-induced lipid accumulation and lipogenic markers via inhibition of protein arginine methyltransferase-3 in AML12 cells and mouse primary hepatocytes (Park et al., 2015). Other studies have suggested a positive relation between irisin and lipid dysfunction. Circulating irisin levels were positively associated with total cholesterol, LDL cholesterol and fasting fatty acids in a Chinese population independent of BMI (Tang et al., 2015) and in women with polycystic ovary syndrome (Li et al., 2015b). Energy restriction induced depletion of irisin was associated with decrease in total cholesterol, total cholesterol/HDL-cholesterol

Abbreviations: DIO, high fat diet-induced obese; AMPK, 5′ AMP-activated protein kinase; SREBP2, sterol regulatory element-binding transcription factor 2; FNDC5, fibronectin type β domain containing 5; OA, oleic acid; NCD, normal chow diet; HFD, high-fat diet; BW, body weight; WAT, white adipose tissue; CC, compound C; siRNA, small interfering RNA.

* Corresponding author at: Department of Physiology and Pathophysiology, Peking University Health Science Center, Beijing 100191, China.
E-mail addresses: tangyunlian626@126.com (H. Tang), yyyrrrlll@126.com (R. Yu), from_jessica@163.com (S. Liu), tafcalgen@163.com (B. Huwatibieke), liziru@umich.edu (Z. Li), weizhenz@umich.edu (W. Zhang).

http://dx.doi.org/10.1016/j.ebiom.2016.02.041

ratio, LDL-cholesterol and apolipoprotein B, independent of changes in body weight (de la Iglesia et al., 2014). In adults at higher cardiovascular risk, irisin was negatively associated with HDL cholesterol and large HDL particles (Panagiotou et al., 2014). In addition, serum irisin was significantly higher in patients with nonalcoholic fatty liver disease (Choi et al., 2014) and in patients with portal inflammation (Polyzos et al., 2014). Moreover, plasma irisin was positively related to total cholesterol in adults with Prader–Willi Syndrome (Hirsch et al., 2015). Nevertheless, other studies have found no significant association of irisin with raised triglyceride and reduced HDL in obese adults with metabolic syndrome (Yan et al., 2014) or with NAFLD (Polyzos et al., 2015). In addition, irisin has been demonstrated to exercise no effect on either lipolysis in 3T3-L1 adipocytes or fatty acid metabolism in HepG2 hepatocytes (Wang et al., 2015). Therefore, further investigation is necessary to define the role of irisin in lipid metabolism.

Here we reported that irisin suppressed cholesterol synthesis in hepatocytes through the activation of 5′ AMP-activated protein kinase (AMPK) and subsequent inhibition of transcription and nuclear translocation of sterol regulatory element-binding transcription factor 2 (SREBP2).

2. Materials and Methods

2.1. Materials

Antibodies used in the study were: pAMPKα Thr172 (2535, CST, Beverly, MA, USA) and AMPKα (2532, CST), SREBP2 (ab30682, Abcam, Cambridge, MA, USA) and β-actin (AT 0001, Milwaukee, WI). Donkey-anti-rabbit Alexa Fluor® 488-IgG (711-545-152) was from Jackson ImmunoResearch (West Grove, PA, USA). IRDye-conjugated affinity purified anti-rabbit and anti-mouse IgGs were purchased from Rockland (Gilbertsville, PA, USA). Irisin (067-16) was from Pheonix (Burlingame, CA, USA). Recombinant irisin-Fc and Fc control were expressed in HEK293 cells (Abgent, Nanjing, China) and purified by high-performance liquid chromatography. Oleic acid (OA), collagenase IV and compound C were purchased from Sigma Aldrich (St. Louis, MO, USA). Alzet microosmotic pumps (1002) were from DURECT Corporation (Cupertino, CA, USA). Aprotinin was purchased from Amersham Biosciences (Pittsburgh, PA, USA). Triglyceride and cholesterol Colorimetric Assay Kits were from Cayman Chemical Company (Ann Arbor, MI, USA). BCA protein quantitative assay kit was from Applied Gene (Beijing, China).

2.2. Animals

Animals were handled in accordance with the Guide for the Care and Use of Laboratory Animals published by the US National Institutes of Health (NIH publication no. 85-23, revised 1996). All experimental protocols were approved by the Animal Care and Use Committee of Peking University. Mice were housed in standard plastic rodent cages and maintained in a regulated environment (24 °C, 12-h light and 12-h dark cycle with lights on at 7 AM and off at 7 PM). Four-week-old male C57BL/6J mice were fed a normal chow diet (NCD) or a high-fat diet (HFD) (60% fat, D12492; Research Diets, New Brunswick, NJ, USA) ad libitum for 14 weeks followed by 2-week subcutaneous perfusion of irisin-Fc or Fc control at a dose of 12 nmol/d·kg body weight (BW). Food intake was measured and averaged for 2 mice in one cage. Mice were sacrificed without fasting after anesthesia by intraperitoneal injection of pentobarbital sodium at 70 mg/kg BW. Liver was frozen in liquid nitrogen and stored in −80 °C freezer for future experiments. Blood samples were transcardially collected and immediately transferred to chilled polypropyrene tubes containing EDTA-Na_2 (12.5 mg/mL) and aprotinin (1000 units/mL) and centrifuged at 4 °C. The plasma was separated and stored at −80 °C before use.

2.3. Implantation of Osmotic Minipumps

The minipumps were placed in a Petri dish with sterile 0.9% saline at 37 °C for at least 4 h, then filled with the test agent before implantation. Mice were anesthetized with pentobarbital sodium and a 1 cm incision was made in the back skin through which an Alzet osmotic minipump (model 1002) filled with irisin-Fc or Fc control was implanted subcutaneously.

2.4. Isolation and Culture of Primary Hepatocytes

Twelve-week old lean or diet-induced-obese (DIO) C57BL/6J mice were anesthetized with pentobarbital sodium at 60 mg/kg BW and injected intraperitoneally with 1000 IU heparin. After laparotomy, the portal vein was cannulated. The liver was perfused with 20 mL of pre-warmed 37 °C Hanks buffer, followed by 20 mL of 0.02% collagenase IV at a flow rate of 2 mL/min. After perfusion, liver tissues were removed and washed with warm Hanks buffer. Liver capsule was removed, and hepatic tissues dispersed and incubated in 20 mL of 0.01% collagenase IV in a shaking water bath at 37 °C for 20 min. Cell suspension was then filtered through 80-μm nylon mesh twice, centrifuged at 500 rpm [SorvallRT7 Benchtop Centrifuge with RTH 250 rotor (Ramsey, MN)] and washed twice with DMEM to remove tissue dissociation enzymes, damaged cells, and nonparenchymal cells. Dispersed hepatocytes were counted and seeded at a concentration of 1–2 × 10^5 cells per well in a 6-well plate containing 2 mL of high glucose DMEM supplemented with 10% (vol/vol) FBS. Cells were cultured at 37 °C in a humidified atmosphere of 5% (vol/vol) CO_2. Culture medium was changed to high glucose DMEM supplemented with 2% (vol/vol) FBS 24 h later. Hepatocytes were then treated with 10 nM irisin for 20 min or 3, 6, 12 and 24 h as indicated in the absence or presence of 125 μM OA. Where indicated, compound C was added 1 h prior to the addition of irisin and OA.

2.5. Cell Culture and siRNA Transfection

HepG2 cells were cultured with high glucose DMEM supplemented with 10% (vol/vol) FBS at 37 °C in a humidified atmosphere of 5% (vol/vol) CO_2. Cells were seeded in a 12-well plate at 30–50% confluency. siRNA was transfected using siRNA-Mate (G04002, GenePharma, Shanghai, China) following the manufacturer's instructions. Culture medium was changed to high glucose DMEM supplemented with 2% (vol/vol) FBS 48 h later. Cells were stimulated with 10 nM irisin for 12 h or 24 h as indicated. siRNA sequences were for Scrambled sense: 5′-UUCUCCGAACGUGUCACGUTT-3′, antisense: 5′-ACGUGACACGUUCG GAGAATT-3′; for siAMPKα1 sense: 5′-CGGGAUCAGUUAGCAACUATT-3′, antisense: 5′-UAGUUGCUAACUGAUCCCGTT-3′.

2.6. Measurements of Triglyceride and Cholesterol Content

Twenty milligram liver tissues were homogenized in 1 mL of 2:1 chloroform/methanol mix on ice and placed at 4 °C for 18 h. Two hundred microliters of distilled water was added to the homogenates. The mixture was vortexed, then centrifuged for 10 min at 3000 rpm, 4 °C. The lower phase was collected, lyophilized and resolved in 5% Triton X-100 in PBS for measurements of lipids. Primary hepatocytes were homogenated according to manufacturer's instructions, and the supernatant was used for lipid detection. Plasma, hepatic and primary hepatocytes triglyceride and cholesterol were measured according to the manufacturer's instructions. Values were normalized to protein concentration.

2.7. Western Blot Analysis

Liver tissues and primary hepatocytes were homogenized in RIPA lysis buffer. Proteins were subjected to SDS/PAGE separation

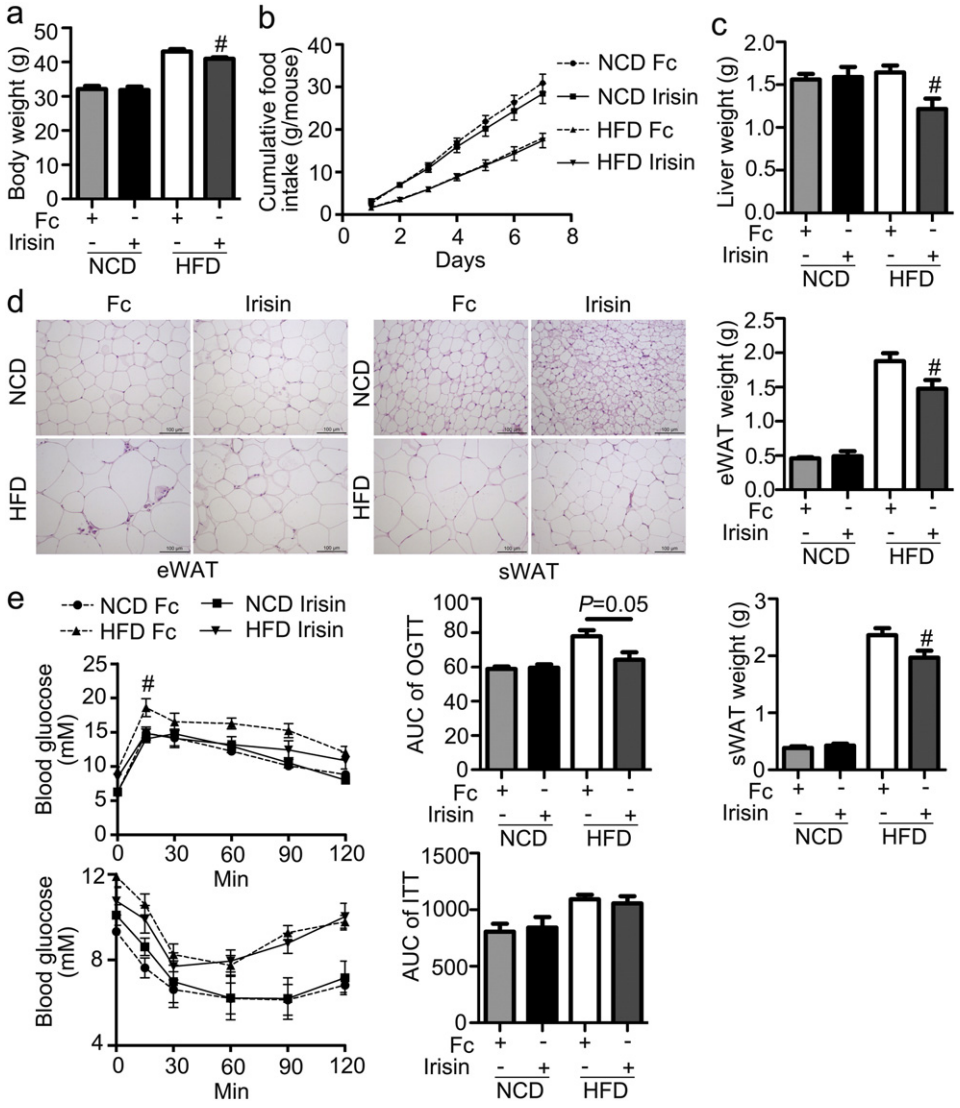

Fig. 1. Effects of irisin on adiposity. Four-week-old C57 BJ/L6 mice were fed NCD or HFD for 16 weeks. During the last 2 weeks, irisin was infused into mice subcutaneously at a dose of 12 nmol/d·kg body weight via an osmotic pump. a. Body weight. b. Cumulative food intake. c. Organ mass. d. HE staining of eWAT and sWAT. e. OGTT and ITT. #$P < 0.05$ vs HFD Fc. $N = 6$.

with a 8–10% running gel, then transferred to a nitrocellulose membrane. Membranes were incubated for 1 h at room temperature with 5% fat-free milk in Tris-buffered saline containing Tween 20, followed by incubation overnight at 4 °C with primary antibodies. Specific reaction was detected by using IRDye-conjugated second antibody and visualized using the Odyssey infrared imaging system (LI-COR Biosciences, Lincoln, NE, USA).

2.8. Gene Expression Analysis

For analyses of gene expression, RNA was extracted from mouse liver or primary hepatocytes using RNATrip (Applied Gene, Beijing, China) and reverse-transcribed into cDNAs using the First-Strand Synthesis System for RT-PCR kit (Fermentas, Lafayette, CO, USA). SYBR Green-based quantitative real time-PCR was performed using the Mx3000 multiplex quantitative PCR system (Stratagene, La Jolla, CA, USA). Triplicate samples were collected for each experiment to determine relative expression levels. All gene expression levels were normalized by β-actin. Sequences for the primer pairs used in this study are listed in Supplemental Table 1.

2.9. Immunofluorescent Staining

Liver frozen sections and isolated hepatocytes were washed with PBS three times and fixed in 4% paraformaldehyde for 20 min, followed by permeabilization with 0.05% Triton X-100 in PBS for 20 min. Nonspecific binding were blocked by 4% goat serum for 1 h. Liver slides or hepatocytes were then incubated with anti-SREBP2 (1:100) overnight at 4 °C. After 3-time wash in PBS, the liver slides or hepatocytes were incubated with anti-rabbit Alex fluor488-conjugated IgG (1:500) at room temperature for 1 h followed by incubation of Hoechst for 15 min. Fluorescent signals were observed and captured under a confocal laser-scanning microscope (Leica). The signal intensity was analyzed by software Leica Qwin 2.6.

2.10. Nuclear Fraction Extraction

Primary hepatocytes cultured in a 6-well plate were washed twice with cold PBS and collected in 100 μL of 1× hypotonic buffer containing 20 mM Tris–HCl of pH 7.4, 10 mM NaCl and 3 mM $MgCl_2$ followed by incubation on ice for 15 min. Five microliter detergent (10% NP40) was added and vortexed for 10 s, then centrifuged for 10 min at 3000 rpm at 4 °C. The supernatant contained the cytoplasmic fraction. The

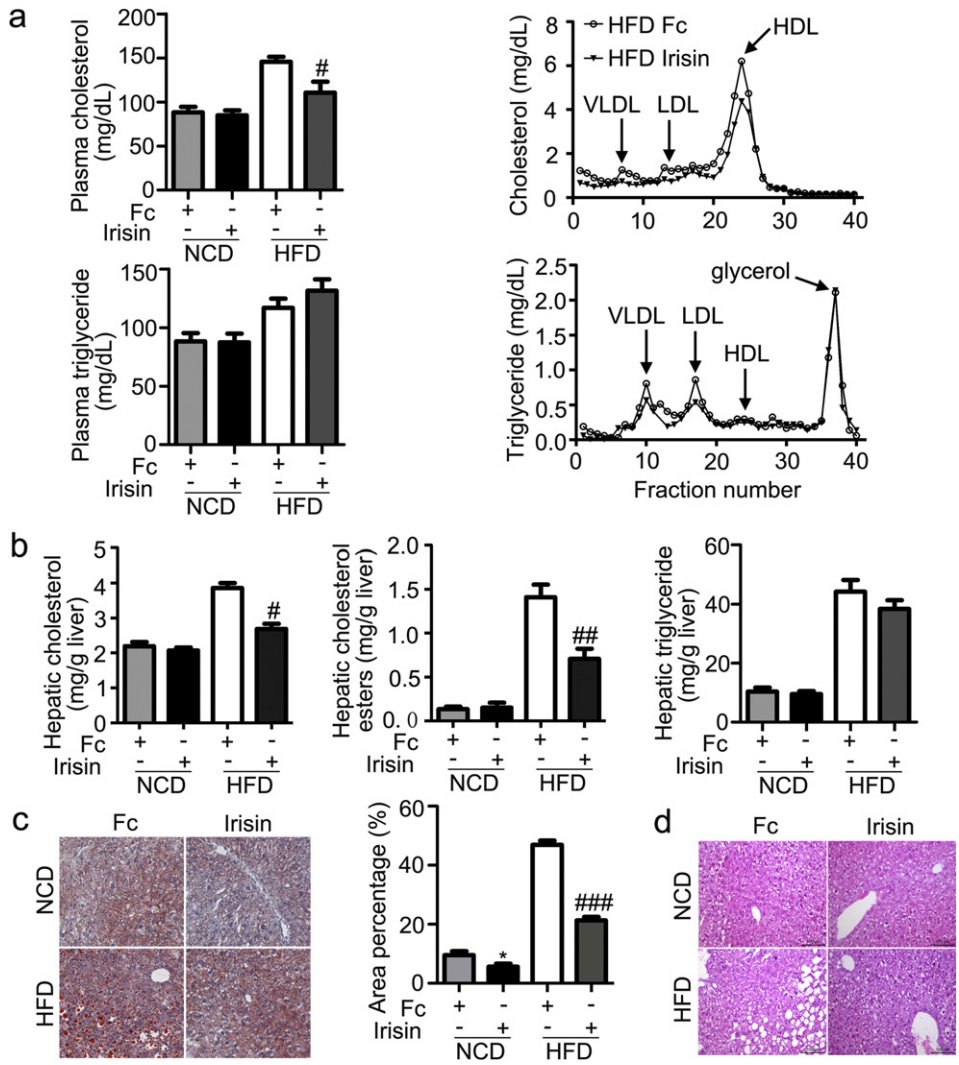

Fig. 2. Effects of irisin on plasma and hepatic lipid contents. C57 BJ/L6 mice fed NCD or HFD for 14 weeks were infused with irisin at a dose of 12 nmol/d·kg body weight for two weeks. a. Plasma cholesterol and triglyceride contents and FPLC-separated lipoprotein fractions. b. Hepatic total and esterified- cholesterol and triglyceride contents. c. Oil red O staining of liver and lipid area quantification. d. HE staining of liver. *$P < 0.05$ vs NCD Fc; #$P < 0.05$, ##$P < 0.01$, ###$P < 0.001$ vs HFD Fc. N = 6. See also Supplemental Fig. 1.

remained nuclear pellets were re-suspended in 50 μL cell extraction buffer (containing 100 mM Tris–HCl of pH 7.4, 2 mM Na_3VO_4, 100 mM NaCl, 1% Triton X-100, 1 mM EDTA, 10% glycerol, 1 mM EGTA, 0.1% SDS, 1 mM NaF, 0.5% deoxycholate and 20 mM $Na_4P_2O_7$) pre-supplemented with 1 mM PMSF and protease inhibitor cocktail and ultrasonicated, followed by centrifugation for 30 min at 14,000 g, 4 °C. Supernatant was collected as the nuclear fraction.

2.11. Fast-protein Liquid Chromatography Fractionation of Lipoproteins

Two hundred microliter of plasma aliquots were pooled from 6 mice per group and applied to Tricorn high-performance Superose S-6 10/300 GL columns using a fast-protein liquid chromatography system (Amersham Biosciences, Marlborough, MA, USA), followed by elution with FPLC buffer (pH 7.4, containing 8.775 g NaCl, 3.58 g $Na_2HPO_4 \cdot 12H_2O$ and 37.2 g EDTA in 1 L distilled water) at a constant flow rate of 0.75 mL/min. Eluted fractions (500 μL) were assayed for triglyceride and cholesterol concentrations.

2.12. Oil Red O Staining

Liver frozen sections were rinsed in PBS three times, then fixed with 4% paraformaldehyde for 10 min. After washing, slices were incubated in 0.3% oil-red staining solution for 1 h at room temperature. Samples were then counterstained with hematoxylin for 30 s, followed by wash in running water for 60 min. All slides were mounted with 90% glycerol and stored at 4 °C before observation. The signal intensity was analyzed by software QWin 2.6.

2.13. Glucose Tolerance Test and Insulin Tolerance Test

For oral glucose tolerance tests, mice were fasted for 16 h followed by intragastric administration of glucose (3 g/kg BW) by gavage. For insulin tolerance tests, mice were fasted for 6 h, followed by intraperitoneal injection of insulin (1 IU/kg BW). Blood was drawn from the tail vein at 0, 15, 30, 60, 90 and 120 min, and blood glucose concentrations were detected immediately.

2.14. Statistical Analysis

All data are expressed as mean ± SEM. Statistical difference was determined by Student's t test or two-way ANOVA and post-hoc Bonferroni test. $P < 0.05$ was considered significant.

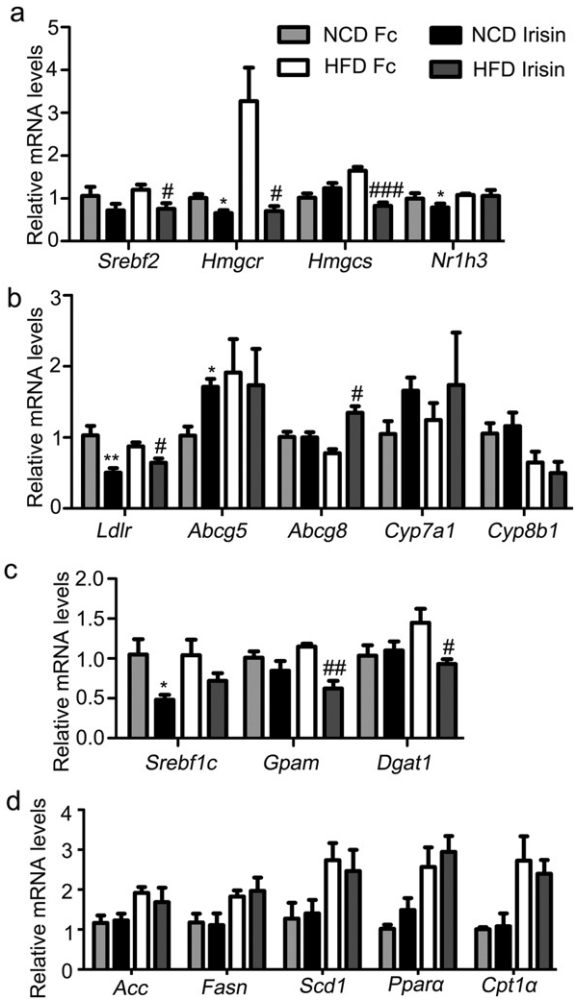

Fig. 3. Effects of irisin on cholesterol metabolism related genes in mouse liver. Four-week-old C57 BJ/L6 mice were fed NCD or HFD for 16 weeks. During the last 2 weeks, irisin was infused into mice subcutaneously at a dose of 12 nmol/d·kg body weight via an osmotic pump. Hepatic mRNA expression was analyzed via real-time PCR. a. mRNA levels of cholesterol synthesis related genes. b. mRNA levels of cholesterol transport and degradation related genes. c. mRNA levels of triglyceride synthesis related genes. d. mRNA levels of fatty acid synthesis and oxidation related genes. $^{*}P < 0.05$, $^{**}P < 0.01$ vs NCD Fc; $\#P < 0.05$, $\#\#P < 0.01$, $\#\#\#P < 0.001$ vs HFD Fc. N = 6.

3. Results

3.1. Amelioration of Obesity by Irisin

Four-week-old C57 BJ/L6 mice were fed NCD or HFD for 16 weeks. During the last 2 weeks, irisin was infused into mice subcutaneously at a dose of 12 nmol/d·kg BW via an osmotic pump. As shown in Fig. 1, irisin decreased body weight of DIO mice relative to animals receiving vehicle control (Fig. 1a), while demonstrated no effect on food intake (Fig. 1b). Organ mass for liver, epididymal white adipose tissue (eWAT) and subcutaneous WAT (sWAT) was also decreased by irisin in DIO mice (Fig. 1c). The reduction in WAT mass was associated with a decrease in the size of adipocytes in eWAT and sWAT, especially in the DIO group (Fig. 1d), as well as induction of multilocular lipid droplets in adipocytes in animals fed NCD (Fig. 1d). Interestingly, glucose intolerance in DIO mice was ameliorated by irisin, whereas insulin sensitivity remained unaltered (Fig. 1e).

3.2. Effect of Irisin on Plasma and Hepatic Cholesterol Contents

Since irisin improved adiposity in mice, we next examined the change of lipid levels. As shown in Fig. 2, irisin significantly decreased plasma total, VLDL-, LDL-, HDL-cholesterol, and hepatic levels of total and esterified cholesterol in DIO mice, while demonstrated no consistent effect on plasma and hepatic triglyceride (Fig. 2a, b). Consistently, Oil red O staining showed reduced fat deposition in hepatocytes in mice treated with irisin relative to the control (Fig. 2c). Histological examination demonstrated a significant reduction of vacuolation in the liver of DIO mice (Fig. 2d). Similar results were observed for synthetic irisin (Supplemental Fig. 1). Collectively, irisin reduced plasma and hepatic cholesterol contents in DIO mice.

3.3. Effect of Irisin on Cholesterol Metabolism Related Genes in Mouse Liver

Genes related to lipid synthesis, transport and degradation in the liver were next determined. As shown in Fig. 3a, mRNA levels of SREBP2 (*Srebf2*), 3-hydroxy-3-methylglutaryl-CoA reductase (*Hmgcr*), 3-hydroxy-3-methylglutaryl-Coenzyme A synthase (*Hmgcs*) and the liver X receptor α (LXRα, *Nr1h3*)), which are all important in cholesterol synthesis, were significantly decreased by irisin treatment. In addition, peripheral infusion of irisin significantly suppressed mRNA levels of low density lipoprotein receptor (*Ldlr*) that recognizes and uptakes LDL-cholesterol, while increased mRNA levels of ATP-binding cassette gene 5 (*Abcg5*) and *Abcg8* which form a heterodimer to mediate cholesterol secretion (Fig. 3b). No significant effect was observed for *Cyp7a1* and *Cyp8b1* which are critical for bile acid synthesis from cholesterol (Fig. 3b). Further, no change in *Fgf21* mRNA expression (Supplemental Fig. 2a) and AKT phosphorylation (Supplemental Fig. 2b) were detected after irisin infusion. As for genes related to triglyceride metabolism, irisin demonstrated only modest inhibition for triglyceride synthesis-related genes such as SREBP1c (*Srebf1c*), glycerol-3-phosphate acyltransferase (*Gpam*), and diacylglycerol O-acyltransferase 1 (*Dgat1*) (Fig. 3c). mRNA levels of genes critical for fatty acid synthesis including acetyl-Coenzyme A carboxylase alpha (*Acaca*), fatty acid synthase (*Fasn*), and stearoyl-Coenzyme A desaturase 1 (*Scd1*), and β-oxidation such as peroxisome proliferator-activated receptor α (*Pparα*) and carnitine palmitoyltransferase 1A (*Cpt1α*) remained unchanged (Fig. 3d). Therefore, irisin decreased mRNA expression of genes related to the synthesis of cholesterol, while increased those genes related to cholesterol excretion.

3.4. Direct Effects of Irisin on Cholesterol Synthesis in Cultured Primary Hepatocytes

To determine whether irisin directly acts on hepatocytes to regulate cholesterol synthesis, we treated the primary hepatocytes isolated from either lean (Fig. 4a–d) or DIO (Fig. 4e–g) mice with irisin. OA was previously reported to increase cholesterol synthesis and HMGCR activity in hepatocytes (Goh and Heimberg, 1976; Gibbons et al., 1986). We thus treated the cultured hepatocytes with OA in our experiment. OA-induced increase in cholesterol content was reversed by irisin treatment in primary hepatocytes from either lean (Fig. 4a) or DIO (Fig. 4e) mice, while no significant change was observed for triglyceride in hepatocytes from DIO mice (Fig. 4e). We next examined the mRNA expression of genes related to cholesterol metabolism in hepatocytes from lean mice. Consistent with the alteration in mouse liver, mRNA levels of *Srebf2*, *Hmgcr*, *Hmgcs* and *Ldlr* were decreased by irisin treatment in the presence or absence of OA in cultured hepatocytes (Fig. 4b). However, mRNA levels of *LXRα*, *Abcg5*, *Abcg8*, *Cyp7a1* and *Cyp8b1* were not affected (Fig. 4c). mRNA levels of genes related to triglyceride metabolism including *Srebf1c*, *Dgat1*, and *Cpt1α* were not affected (Fig. 4d). Similar observation was detected in hepatocytes from DIO mice. mRNA levels of *Srebf2*, *Hmgcr*, *Hmgcs* and *LXRα* were decreased by treatment of hepatocytes with irisin in the presence or absence of OA (Fig. 4f). However, genes related to cholesterol uptake (*Ldlr*, *Pcsk9* and *ApoB*), secretion (*Abca1*, *Abcg5* and *Abcg8*) and bile acid synthesis (*Cyp7a1* and *Cyp8b1*) remained largely unaltered (Fig. 4g). Furthermore, conditioned medium from C2C12 myotubes infected with Ad-FNDC5 blocked the OA-induced

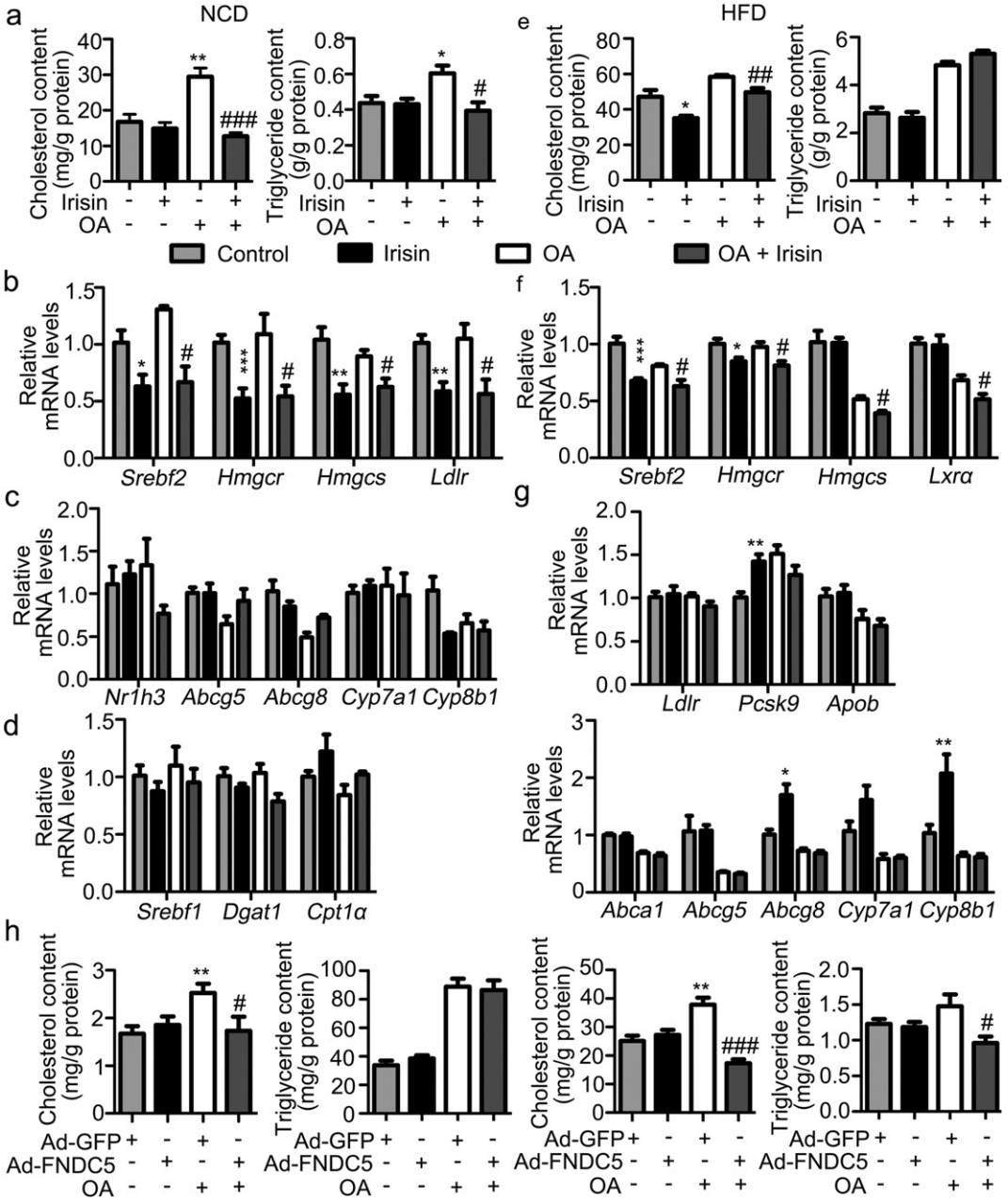

Fig. 4. Direct effects of irisin on cholesterol synthesis in cultured primary hepatocytes. Primary hepatocytes were isolated from either lean (Fig. 4A–D) or DIO (Fig. 4E–G) mice and treated with irisin (10 nM) in the presence or absence of OA (125 μM) for 24 h. a. Cholesterol and triglyceride contents in primary hepatocytes from lean mice. b–d. mRNA levels of genes related to cholesterol synthesis (b), transport and degradation (c), triglyceride synthesis, fatty acid synthesis and β-oxidation (d) in hepatocytes from lean mice. e. Cholesterol and triglyceride contents in primary hepatocytes from DIO mice. f and g. mRNA levels of genes related to cholesterol synthesis (f), transport and degradation (g) in hepatocytes from DIO mice. $^{*}P < 0.05$, $^{**}P < 0.01$, $^{***}P < 0.001$ vs control; $\#P < 0.05$, $\#\#P < 0.01$, $\#\#\#P < 0.001$ vs OA. h. Primary hepatocytes were treated with conditioned medium from C2C12 myotubes infected with Ad-GFP or Ad-FNDC5 for 24 h. Cholesterol and triglyceride contents were measured. $^{**}P < 0.01$ vs Ad-GFP; $\#P < 0.05$, $\#\#\#P < 0.001$ vs Ad-GFP + OA. Shown is the representative of at least 3 experiments.

increment of cholesterol in hepatocytes isolated from either lean or DIO mice, while demonstrated negligible effect on triglyceride (Fig. 4h). All these results indicated that irisin inhibited the cholesterol synthesis in hepatocytes.

3.5. AMPK-SREBP2 Dependent Effects

AMPK-SREBP2 signaling is critical for the regulation of cholesterol metabolism (Quan et al., 2013; Elhanati et al., 2013). We thus investigated whether this signaling mechanism mediates the suppression of cholesterol synthesis induced by irisin in hepatocytes. As shown in Fig. 5a, irisin at a dose of 10 nM significantly increased the phosphorylation of AMPKα Thr172 in a time-dependent manner. This alteration was associated with a decrease in the nuclear translocation of SREBP2 in hepatocytes isolated from mice fed either NCD (Fig. 5b, c) or HFD (Fig. 5d, e).

To determine whether AMPK is required for the effects of irisin on cholesterol synthesis in hepatocytes, compound C was used to block the activation of AMPK. As shown in Fig. 6a, treatment of hepatocytes with compound C for 1 h dose-dependently blocked the activation of AMPK induced by irisin. The blockade of AMPK subsequently reversed irisin-induced reduction of cholesterol contents in hepatocytes isolated from both lean and DIO mice (Fig. 6b). Again, triglyceride was not affected by irisin despite that it was dose-dependently increased by compound C (Fig. 6b). Compound C at a dose of 10 μM was used in the

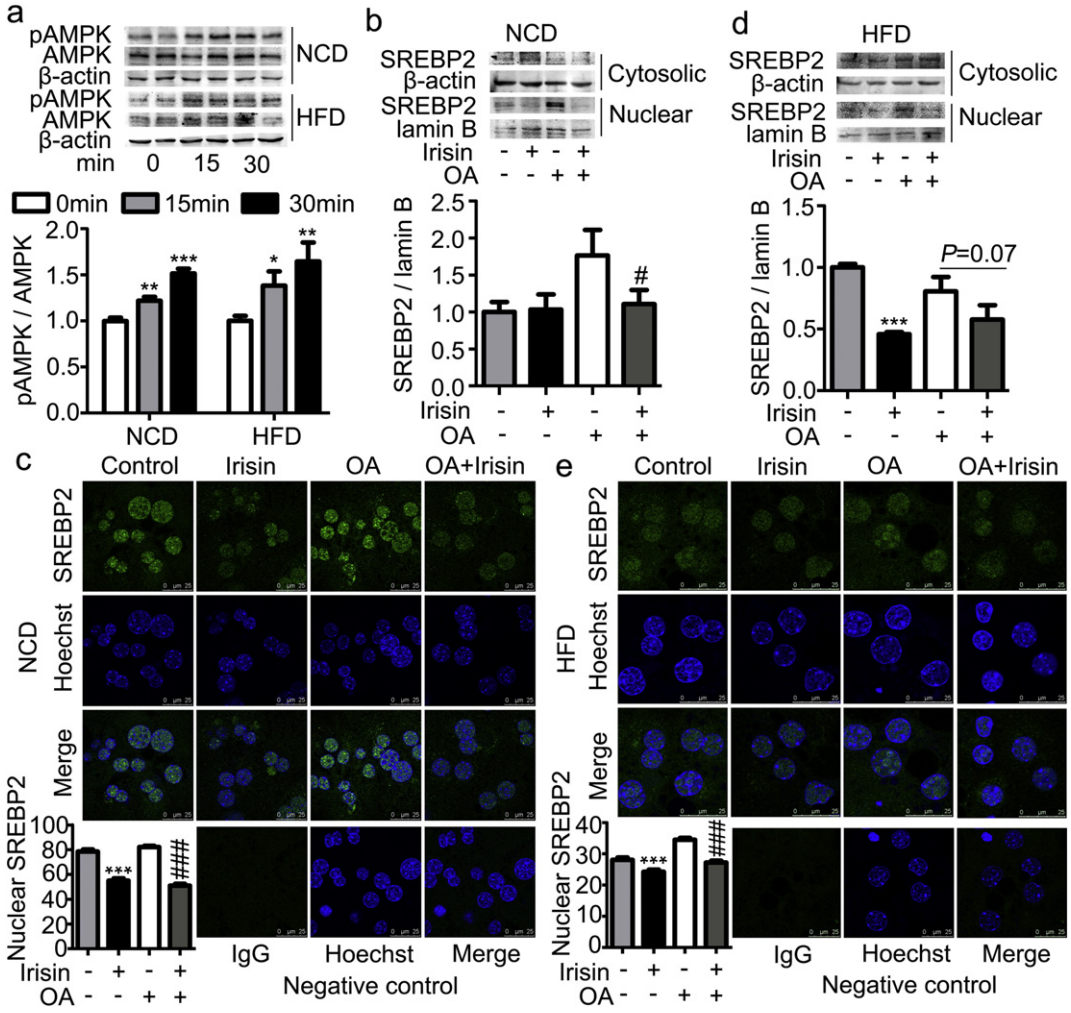

Fig. 5. Effects of irisin on AMPKα and SREBP2 in primary hepatocytes. Primary hepatocytes were isolated from either lean or DIO mice and treated with irisin (10 nM) in the presence or absence OA (125 μM). a. Time-dependent effect of irisin on AMPKα phosphorylation. b. SREBP2 content of cytosolic and nuclear fractions of hepatocytes from lean mice analyzed via Western blot. c. Immunofluorescent staining of hepatocytes from lean mice. d. SREBP2 content of cytosolic and nuclear fractions of hepatocytes from DIO mice analyzed via Western blot. e. Immunofluorescent staining of hepatocytes from DIO mice. ***$P < 0.001$ vs blank control; ###$P < 0.001$ vs OA. Shown is the representative of at least 3 experiments.

rest of experiments. Consistently, compound C reversed the inhibitory effects of irisin on mRNA levels of *Srebf2*, *Hmgcr and Hmgcs* (Supplemental Fig. 3). As shown in Fig. 6c and d, blockade of AMPK activity by compound C completely attenuated the inhibition of SREBP2 nuclear translocation induced by irisin in the presence or absence of OA as revealed by Western blot analysis of the cytosolic and nuclear fractions of hepatocyte proteins and immunofluorescent staining. Consistently, knockdown of AMPKα1 abolished the repression of nuclear SREBP2 translocation (Fig. 7a) and cholesterol accumulation (Fig. 7b) evoked by irisin in HepG2 cells. Consistently, the inhibitory effect of irisin on mRNA expression of *SREBF2*, *HMGCR* and *HMGCS* was significantly blocked by inhibition of AMPK by AMPKα1 knockdown (Fig. 7c). Therefore, blockade of irisin-induced activation of AMPK reversed its inhibition on SREBP2 nuclear translocation and subsequent suppression of cholesterol synthesis.

4. Discussion

Our study demonstrated that irisin could inhibit hepatic cholesterol synthesis via AMPK-dependent inhibition of SREBP2 and its downstream target genes. Irisin increased the phosphorylation of AMPKα in hepatocytes. Blockage of irisin-induced AMPK activation by compound C or knockdown of AMPKα1 reversed the suppressive effects of irisin on: 1) hepatic cholesterol synthesis; 2) mRNA expression of SREBP2 and its downstream target genes critical for cholesterol synthesis; and 3) nuclear translocalization of SREBP2.

Previous studies have indicated that irisin could improve dyslipidemia and hepatic steatosis in mice (Xiong et al., 2015). The decrement of lipid accumulation in hepatocytes was proposed to result mainly from the suppression of triglyceride synthesis (Park et al., 2015). In cultured AML12 hepatocytes, recombinant irisin significantly reduced the PA-induced lipid accumulation, and inhibited the PA-induced increase in lipogenic markers ACC and FAS at the mRNA and protein levels (Park et al., 2015). Our studies identified suppression of cholesterol synthesis as an alternative pathway for irisin to reduce lipid content in hepatocytes. This conclusion is supported by following observations: 1) Administration of irisin reduced the hepatic lipid contents measured by Oil-red staining in lean and obese mice; 2) In mice and cultured hepatocytes, irisin decreased levels of hepatic cholesterol, while demonstrated no effect on triglyceride contents; 3) Irisin inhibited SREBP2 and its target genes HMGCS2 and HMGCR, a key transcriptional factor and the rate-limiting enzymes for cholesterol synthesis respectively; 4) The effects of irisin on genes related to triglyceride synthesis and β-oxidation were negligible in hepatocytes. There exist two possible explanations for the conflicting observations: different cell models and sources of irisin used. In the studies by Park et al. (Park et al., 2015), AML12 mouse hepatocyte cell line was used. This cell line expresses high levels of human transforming growth factor α (TGFα). Whether

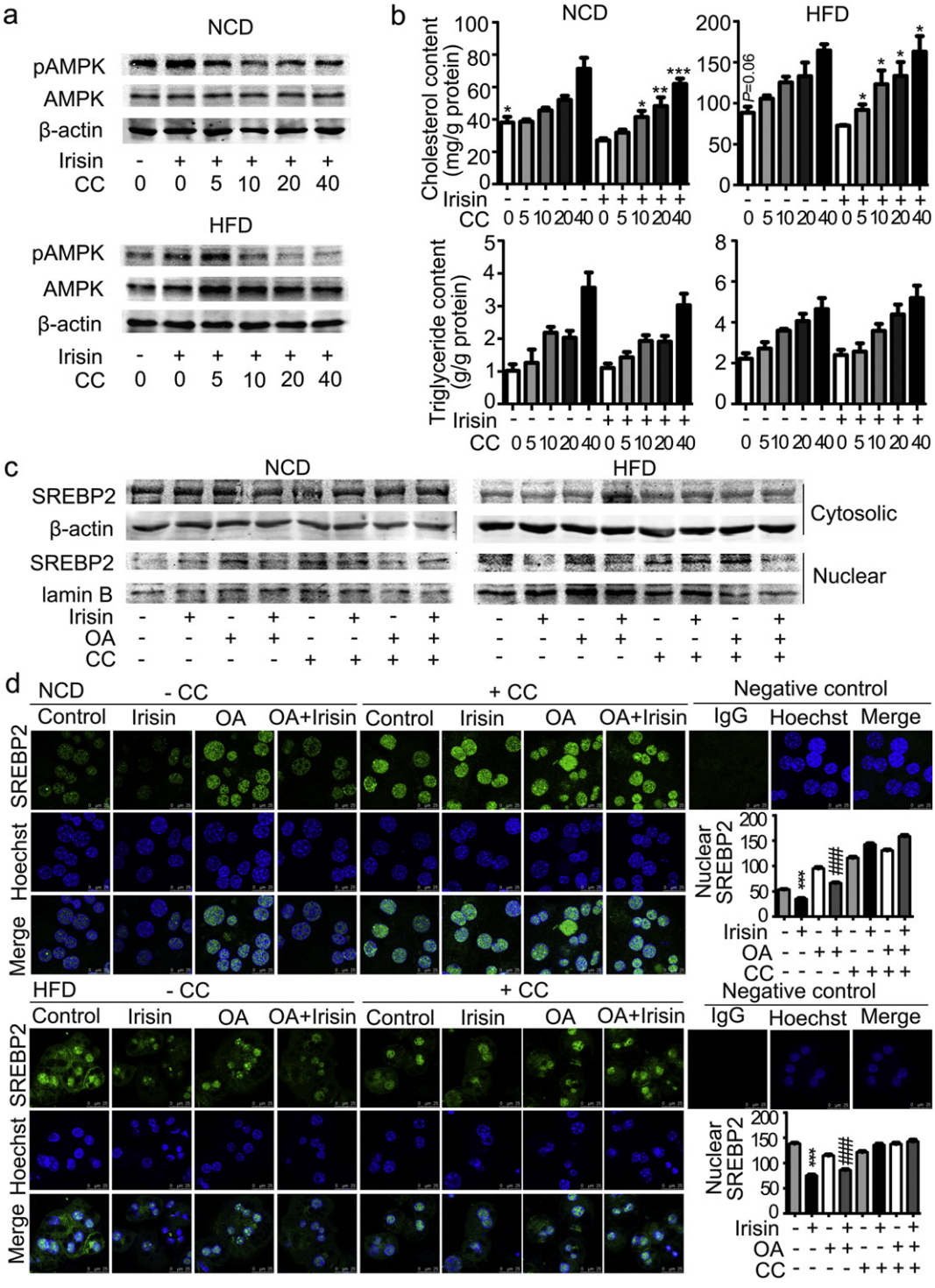

Fig. 6. Compound C blocked the effects of irisin on AMPKα and SREBP2. Primary hepatocytes were isolated from either lean or DIO mice and treated with compound C for 1 h prior to the addition of irisin (10 nM) with or without OA (125 μM). a. Compound C dose-dependently reversed the phosphorylation of AMPKα induced by irisin. b. Cholesterol and triglyceride contents in hepatocytes after compound C and irisin treatment. $^{*}P < 0.05$, $^{**}P < 0.01$, $^{***}P < 0.001$ vs irisin. c. SREBP2 contents of cytosolic and nuclear fractions of hepatocytes treated with compound C, irisin and/or OA. d. Immunofluorescent staining of SREBP2 in hepatocytes treated with compound C, irisin and/or OA. $^{***}P < 0.001$ vs vehicle control; $^{###}P < 0.001$ vs OA. Shown is the representative of 3 experiments. CC, compound C.

the high expression of TGFα in AML12 cells accounts for the distinct response to irisin remains to be explored. Theoretically, the preparation of irisin may affect its biological functions. This potential is unlikely because we observed no difference in the suppression of cholesterol synthesis between recombinant irisin-Fc and synthetic irisin.

While good progress has been made in identifying the physiological actions of irisin, its receptor and intracellular signaling pathway remains largely unknown. Previous studies have shown that irisin may activate AMPK, PI3K/AKT, or p38 MAPK and ERK (Liu et al., 2015b; Yang et al., 2015; Zhang et al., 2014; Lee et al., 2015) in skeletal muscle cells, hepatocytes and adipocytes. Our studies also suggest the presence of a functional receptor for irisin in hepatocytes. Activation of this receptor by irisin may stimulate AMPK activity, leading to the subsequent suppression of SREBP2 expression and nuclear translocalization. This

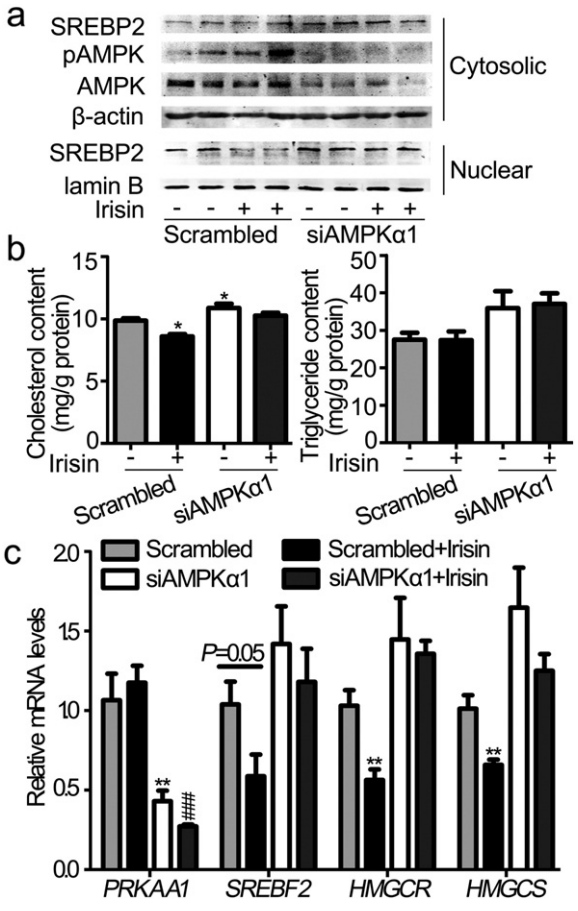

Fig. 7. Knockdown of AMPKα1 abolished the effects of irisin on cholesterol synthesis in HepG2 cells. HepG2 cells were transfected with siAMPKα1 and stimulated with irisin (10 nM) 48 h later. a. HepG2 cells were treated with irisin for 12 h. Cytosolic and nuclear proteins were analyzed by Western blot. b. HepG2 cells were stimulated with irisin for 24 h and measured for cholesterol and triglyceride content. c. HepG2 cells were stimulated with irisin for 24 h. mRNA levels of *PRKAA1* (AMPKα1) and cholesterol synthesis related genes were analyzed by real-time PCR. $^{*}P < 0.05$, $^{**}P < 0.01$ vs Scrambled; $^{\#\#\#}P < 0.001$ vs Scrambled + Irisin. Shown is the representative of 3 experiments.

observation is consistent with previous report demonstrating that AMPK could phosphorylate SREBP2 to reduce SREBP2 precursor cleavage and nuclear translocalization (Liu et al., 2015a). Although activation of AMPK has been demonstrated to suppress hepatic lipid synthesis and to promote fatty acid β-oxidation by phosphorylating SREBP1c (Liu et al., 2015a; Ma et al., 2015; Elhanati et al., 2013; Samovski et al., 2015; Chen et al., 2014; Lee et al., 2012), our studies did not detect consistent change in the levels of triglyceride, SREBP1c and its downstream target genes. A much higher dose of irisin may be required for its effect on triglyceride synthesis. Instead, SREBP2 transcription and nuclear translocalization in hepatocytes were significantly attenuated upon activation of AMPK by irisin. The molecular mechanism underlying the selection of SREBP2 over SREBP1 upon activation of irisin receptor in hepatocytes is currently unknown.

Emerging evidence has indicated that cross talks between organs are critical for energy homeostasis. The present studies suggest a direct communication between the skeletal muscle and liver via irisin. Our study also provides significant evidence that hepatocytes are targets for irisin in term of the regulation of hepatic cholesterol metabolism. Conditioned medium from C2C12 myocytes overexpressing FNDC5 significantly attenuated cholesterol synthesis in cultured hepatocytes. Other studies also support the concept that irisin may serve as an important cross-organ messenger linking skeletal muscle with the brain, adipose tissue and the cardiovascular system to integrate the exercise with the physiological activities in these organs (Wrann et al., 2013; Huh et al., 2014; Xiong et al., 2015; Song et al., 2014; Wu et al., 2015; Zhu et al., 2015; Zhang et al., 2015). Importantly, irisin acts in concert with fibroblast growth factor 21 to promote adipocyte browning and thermogenesis in humans (Lee et al., 2014). This result indicates that cross talk between skeletal muscle and adipose tissue may be critical for the control of adiposity. Taken together, all these observations suggest that irisin is an important molecule linking the skeletal muscle with the adipose tissue and liver to integrate lipid metabolism.

Despite the significant reduction in hepatic cholesterol, irisin at the dose used in the study demonstrates no effect on the insulin sensitivity in either lean or high fat diet induced obese mice. The mechanism underlying the dissociation effects of irisin on hepatic cholesterol and glucose metabolism is currently unknown. Whether the dose of irisin contributes to this discrepancy remains to be explored.

In conclusion, our studies indicate that irisin inhibits hepatic cholesterol synthesis via the mechanism dependent of AMPK-SREBP2 signaling. This finding may shed light on the treatment of diseases related to hypercholesterolemia, such as atherosclerosis.

Author Contributions

Z. W. conceived of and designed the experiments. T. H., Y. R., L. S., and H. B. conducted the experiments. T. H. analyzed and interpreted the data. L. Z. assisted in preparing the ad-FNDC5 adenovirus. T. H. and Z. W. wrote the manuscript.

Funding Sources

This research was funded by National Natural Science Foundation of China grants 81330010 and 81390354, and American Diabetes Association grant #1-13-BS-225. Our funding sources had no role in data collection, analysis or interpretation, and were not involved in the writing of this manuscript.

Conflict of Interest Statement

The authors declare no conflict of interests.

Acknowledgments

We thank Guoqing Liu for assistance in FPLC, Nanping Wang for the Ad-GFP adenovirus, and Bruce Spiegelman for the Ad-FNDC5 adenovirus.

Appendix A. Supplementary Data

Supplementary data to this article can be found online at http://dx.doi.org/10.1016/j.ebiom.2016.02.041.

References

Aronis, K.N., Moreno, M., Polyzos, S.A., Moreno-Navarrete, J.M., Ricart, W., Delgado, E., De La Hera, J., Sahin-Efe, A., Chamberland, J.P., Berman, R., Spiro III, A., Vokonas, P., Fernandez-Real, J.M., Mantzoros, C.S., 2015. Circulating irisin levels and coronary heart disease: association with future acute coronary syndrome and major adverse cardiovascular events. Int. J. Obes. 39, 156–161.

Bilski, J., Mazur-Bialy, A.I., Brzozowski, B., Magierowski, M., Jasnos, K., Krzysiek-Maczka, G., Urbanczyk, K., Ptak-Belowska, A., Zwolinska-Wcislo, M., Mach, T., Brzozowski, T., 2015. Moderate exercise training attenuates the severity of experimental rodent colitis: the importance of crosstalk between adipose tissue and skeletal muscles. Mediat. Inflamm. 2015, 605071.

Bostrom, P., Wu, J., Jedrychowski, M.P., Korde, A., Ye, L., Lo, J.C., Rasbach, K.A., Bostrom, E.A., Choi, J.H., Long, J.Z., Kajimura, S., Zingaretti, M.C., Vind, B.F., Tu, H., Cinti, S., Hojlund, K., Gygi, S.P., Spiegelman, B.M., 2012. A PGC1-alpha-dependent myokine that drives brown-fat-like development of white fat and thermogenesis. Nature 481, 463–468.

Chen, L., Shu, Y., Liang, X., Chen, E.C., Yee, S.W., Zur, A.A., Li, S., Xu, L., Keshari, K.R., Lin, M.J., Chien, H.C., Zhang, Y., Morrissey, K.M., Liu, J., Ostrem, J., Younger, N.S., Kurhanewicz, J., Shokat, K.M., Ashrafi, K., Giacomini, K.M., 2014. OCT1 is a high-capacity thiamine transporter that regulates hepatic steatosis and is a target of metformin. Proc. Natl. Acad. Sci. U. S. A. 111, 9983–9988.

Choi, E.S., Kim, M.K., Song, M.K., Kim, J.M., Kim, E.S., Chung, W.J., Park, K.S., Cho, K.B., Hwang, J.S., Jang, B.K., 2014. Association between serum irisin levels and non-alcoholic fatty liver disease in health screen examinees. PLoS One 9, e110680.
Choi, Y.K., Kim, M.K., Bae, K.H., Seo, H.A., Jeong, J.Y., Lee, W.K., Kim, J.G., Lee, I.K., Park, K.G., 2013. Serum irisin levels in new-onset type 2 diabetes. Diabetes Res. Clin. Pract. 100, 96–101.
De La Iglesia, R., Lopez-Legarrea, P., Crujeiras, A.B., Pardo, M., Casanueva, F.F., Zulet, M.A., Martinez, J.A., 2014. Plasma irisin depletion under energy restriction is associated with improvements in lipid profile in metabolic syndrome patients. Clin. Endocrinol. 81, 306–311.
Duran, I.D., Gulcelik, N.E., Unal, M., Topcuoglu, C., Sezer, S., Tuna, M.M., Berker, D., Guler, S., 2015. Irisin levels in the progression of diabetes in sedentary women. Clin. Biochem.
Ebert, T., Focke, D., Petroff, D., Wurst, U., Richter, J., Bachmann, A., Lossner, U., Kralisch, S., Kratzsch, J., Beige, J., Bast, I., Anders, M., Bluher, M., Stumvoll, M., Fasshauer, M., 2014. Serum levels of the myokine irisin in relation to metabolic and renal function. Eur. J. Endocrinol. 170, 501–506.
Ebert, T., Kralisch, S., Wurst, U., Scholz, M., Stumvoll, M., Kovacs, P., Fasshauer, M., Tonjes, A., 2015. Association of metabolic parameters and rs726344 in FNDC5 with serum irisin concentrations. Int. J. Obes.
Elhanati, S., Kanfi, Y., Varvak, A., Roichman, A., Carmel-Gross, I., Barth, S., Gibor, G., Cohen, H.Y., 2013. Multiple regulatory layers of SREBP1/2 by SIRT6. Cell Rep. 4, 905–912.
Espes, D., Lau, J., Carlsson, P.O., 2015. Increased levels of irisin in people with long-standing type 1 diabetes. Diabet. Med. 32, 1172–1176.
Gibbons, G.F., Attwell Thomas, C.P., Pullinger, C.R., 1986. The metabolic route by which oleate is converted into cholesterol in rat hepatocytes. Biochem. J. 235, 19–24.
Goh, E.H., Heimberg, M., 1976. Effect of oleic acid and cholesterol on the activity of hepatic hydroxymethylglutaryl coenzyme A reductase. FEBS Lett. 63, 209–210.
Hirsch, H.J., Gross, I., Pollak, Y., Eldar-Geva, T., Gross-Tsur, V., 2015. Irisin and the metabolic phenotype of adults with Prader–Willi Syndrome. PLoS One 10, e0136864.
Hou, N., Han, F., Sun, X., 2015. The relationship between circulating irisin levels and endothelial function in lean and obese subjects. Clin. Endocrinol. 83, 339–343.
Huh, J.Y., Dincer, F., Mesfum, E., Mantzoros, C.S., 2014. Irisin stimulates muscle growth-related genes and regulates adipocyte differentiation and metabolism in humans. Int. J. Obes. 38, 1538–1544.
Huh, J.Y., Panagiotou, G., Mougios, V., Brinkoetter, M., Vamvini, M.T., Schneider, B.E., Mantzoros, C.S., 2012. FNDC5 and irisin in humans: I. Predictors of circulating concentrations in serum and plasma and II. mRNA expression and circulating concentrations in response to weight loss and exercise. Metab. Clin. Exp. 61, 1725–1738.
Kurdiova, T., Balaz, M., Vician, M., Maderova, D., Vlcek, M., Valkovic, L., Srbecky, M., Imrich, R., Kyselovicova, O., Belan, V., Jelok, I., Wolfrum, C., Klimes, I., Krssak, M., Zemkova, E., Gasperikova, D., Ukropec, J., Ukropcova, B., 2014. Effects of obesity, diabetes and exercise on Fndc5 gene expression and irisin release in human skeletal muscle and adipose tissue: in vivo and in vitro studies. J. Physiol. 592, 1091–1107.
Lee, H.J., Lee, J.O., Kim, N., Kim, J.K., Kim, H.I., Lee, Y.W., Kim, S.J., Choi, J.I., Oh, Y., Kim, J.H., Suyeon, H., Park, S.H., Kim, H.S., 2015. Irisin, a novel myokine, regulates glucose uptake in skeletal muscle cells via AMPK. Mol. Endocrinol. 29, 873–881.
Lee, J.W., Choe, S.S., Jang, H., Kim, J., Jeong, H.W., Jo, H., Jeong, K.H., Tadi, S., Park, M.G., Kwak, T.H., Man Kim, J., Hyun, D.H., Kim, J.B., 2012. AMPK activation with glabridin ameliorates adiposity and lipid dysregulation in obesity. J. Lipid Res. 53, 1277–1286.
Lee, P., Linderman, J.D., Smith, S., Brychta, R.J., Wang, J., Idelson, C., Perron, R.M., Werner, C.D., Phan, G.Q., Kammula, U.S., Kebebew, E., Pacak, K., Chen, K.Y., Celi, F.S., 2014. Irisin and FGF21 are cold-induced endocrine activators of brown fat function in humans. Cell Metab. 19, 302–309.
Li, D.J., Huang, F., Lu, W.J., Jiang, G.J., Deng, Y.P., Shen, F.M., 2015a. Metformin promotes irisin release from murine skeletal muscle independently of AMP-activated protein kinase activation. Acta Physiol (Oxf.) 213, 711–721.
Li, M., Yang, M., Zhou, X., Fang, X., Hu, W., Zhu, W., Wang, C., Liu, D., Li, S., Liu, H., Yang, G., Li, L., 2015b. Elevated circulating levels of irisin and the effect of metformin treatment in women with polycystic ovary syndrome. J. Clin. Endocrinol. Metab. 100, 1485–1493.
Liu, J.J., Wong, M.D., Toy, W.C., Tan, C.S., Liu, S., Ng, X.W., Tavintharan, S., Sum, C.F., Lim, S.C., 2013. Lower circulating irisin is associated with type 2 diabetes mellitus. J. Diabetes Complicat. 27, 365–369.
Liu, S., Jing, F., Yu, C., Gao, L., Qin, Y., Zhao, J., 2015a. AICAR-induced activation of AMPK inhibits TSH/SREBP-2/HMGCR pathway in liver. PLoS One 10, e0124951.
Liu, T.Y., Shi, C.X., Gao, R., Sun, H.J., Xiong, X.Q., Ding, L., Chen, Q., Li, Y.H., Wang, J.J., Kang, Y.M., Zhu, G.Q., 2015b. Irisin inhibits hepatic gluconeogenesis and increases glycogen synthesis via the PI3K/Akt pathway in type 2 diabetic mice and hepatocytes. Clin. Sci. (Lond.) 129, 839–850.
Lopez-Legarrea, P., De La Iglesia, R., Crujeiras, A.B., Pardo, M., Casanueva, F.F., Zulet, M.A., Martinez, J.A., 2014. Higher baseline irisin concentrations are associated with greater reductions in glycemia and insulinemia after weight loss in obese subjects. Nutr. Diabetes 4, e110.
Ma, W., Ding, H., Gong, X., Liu, Z., Lin, Y., Zhang, Z., Lin, G., 2015. Methyl protodioscin increases ABCA1 expression and cholesterol efflux while inhibiting gene expressions for synthesis of cholesterol and triglycerides by suppressing SREBP transcription and microRNA 33a/b levels. Atherosclerosis 239, 566–570.
Miyamoto-Mikami, E., Sato, K., Kurihara, T., Hasegawa, N., Fujie, S., Fujita, S., Sanada, K., Hamaoka, T., Tabata, I., Iemitsu, M., 2015. Endurance training-induced increase in circulating irisin levels is associated with reduction of abdominal visceral fat in middle-aged and older adults. PLoS One 10, e0120354.
Moreno-Navarrete, J.M., Ortega, F., Serrano, M., Guerra, E., Pardo, G., Tinahones, F., Ricart, W., Fernandez-Real, J.M., 2013. Irisin is expressed and produced by human muscle and adipose tissue in association with obesity and insulin resistance. J. Clin. Endocrinol. Metab. 98, E769–E778.
Panagiotou, G., Mu, L., Na, B., Mukamal, K.J., Mantzoros, C.S., 2014. Circulating irisin, omentin-1, and lipoprotein subparticles in adults at higher cardiovascular risk. Metab. Clin. Exp. 63, 1265–1271.
Park, M.J., Kim, D.I., Choi, J.H., Heo, Y.R., Park, S.H., 2015. New role of irisin in hepatocytes: the protective effect of hepatic steatosis in vitro. Cell. Signal. 27, 1831–1839.
Polyzos, S.A., Kountouras, J., Anastasilakis, A.D., Geladari, E.V., Mantzoros, C.S., 2014. Irisin in patients with nonalcoholic fatty liver disease. Metab. Clin. Exp. 63, 207–217.
Polyzos, S.A., Kountouras, J., Anastasilakis, A.D., Margouta, A., Mantzoros, C.S., 2015. Association between circulating irisin and homocysteine in patients with nonalcoholic fatty liver disease. Endocrine 49, 560–562.
Quan, H.Y., Kim Do, Y., Chung, S.H., 2013. Caffeine attenuates lipid accumulation via activation of AMP-activated protein kinase signaling pathway in HepG2 cells. BMB Rep. 46, 207–212.
Rodriguez, A., Becerril, S., Mendez-Gimenez, L., Ramirez, B., Sainz, N., Catalan, V., Gomez-Ambrosi, J., Fruhbeck, G., 2015. Leptin administration activates irisin-induced myogenesis via nitric oxide-dependent mechanisms, but reduces its effect on subcutaneous fat browning in mice. Int. J. Obes. 39, 397–407.
Samovski, D., Sun, J., Pietka, T., Gross, R.W., Eckel, R.H., Su, X., Stahl, P.D., Abumrad, N.A., 2015. Regulation of AMPK activation by CD36 links fatty acid uptake to beta-oxidation. Diabetes 64, 353–359.
Shan, T., Liang, X., Bi, P., Kuang, S., 2013. Myostatin knockout drives browning of white adipose tissue through activating the AMPK-PGC1alpha-Fndc5 pathway in muscle. FASEB J. 27, 1981–1989.
Song, H., Wu, F., Zhang, Y., Wang, F., Jiang, M., Wang, Z., Zhang, M., Li, S., Yang, L., Wang, X.L., Cui, T., Tang, D., 2014. Irisin promotes human umbilical vein endothelial cell proliferation through the ERK signaling pathway and partly suppresses high glucose-induced apoptosis. PLoS One 9, e110273.
Tang, S., Zhang, R., Jiang, F., Wang, J., Chen, M., Peng, D., Yan, J., Wang, S., Bao, Y., Hu, C., Jia, W., 2015. Circulating irisin levels are associated with lipid and uric acid metabolism in a Chinese population. Clin. Exp. Pharmacol. Physiol.
Vaughan, R.A., Gannon, N.P., Barberena, M.A., Garcia-Smith, R., Bisoffi, M., Mermier, C.M., Conn, C.A., Trujillo, K.A., 2014. Characterization of the metabolic effects of irisin on skeletal muscle in vitro. Diabetes Obes. Metab. 16, 711–718.
Wang, C., Wang, L., Li, W., Yan, F., Tian, M., Wu, C., Qi, L., Wang, X., Song, J., Hou, X., Chen, L., 2015. Irisin has no effect on lipolysis in 3T3-L1 adipocytes or fatty acid metabolism in HepG2 hepatocytes. Endocrine 49, 90–96.
Wen, M.S., Wang, C.Y., Lin, S.L., Hung, K.C., 2013. Decrease in irisin in patients with chronic kidney disease. PLoS One 8, e64025.
Wrann, C.D., White, J.P., Salogiannnis, J., Laznik-Bogoslavski, D., Wu, J., Ma, D., Lin, J.D., Greenberg, M.E., Spiegelman, B.M., 2013. Exercise induces hippocampal BDNF through a PGC-1alpha/FNDC5 pathway. Cell Metab. 18, 649–659.
Wu, F., Song, H., Zhang, Y., Mu, Q., Jiang, M., Wang, F., Zhang, W., Li, L., Li, H., Wang, Y., Zhang, M., Li, S., Yang, L., Meng, Y., Tang, D., 2015. Irisin induces angiogenesis in human umbilical vein endothelial cells in vitro and in zebrafish embryos in vivo via activation of the ERK signaling pathway. PLoS One 10, e0134662.
Wu, J., Bostrom, P., Sparks, L.M., Ye, L., Choi, J.H., Giang, A.H., Khandekar, M., Virtanen, K.A., Nuutila, P., Schaart, G., Huang, K., Tu, H., Van Marken Lichtenbelt, W.D., Hoeks, J., Enerback, S., Schrauwen, P., Spiegelman, B.M., 2012. Beige adipocytes are a distinct type of thermogenic fat cell in mouse and human. Cell 150, 366–376.
Wu, M.V., Bikopoulos, G., Hung, S., Ceddia, R.B., 2014. Thermogenic capacity is antagonistically regulated in classical brown and white subcutaneous fat depots by high fat diet and endurance training in rats: impact on whole-body energy expenditure. J. Biol. Chem. 289, 34129–34140.
Xiang, L., Xiang, G., Yue, L., Zhang, J., Zhao, L., 2014. Circulating irisin levels are positively associated with endothelium-dependent vasodilation in newly diagnosed type 2 diabetic patients without clinical angiopathy. Atherosclerosis 235, 328–333.
Xiong, X.Q., Chen, D., Sun, H.J., Ding, L., Wang, J.J., Chen, Q., Li, Y.H., Zhou, Y.B., Han, Y., Zhang, F., Gao, X.Y., Kang, Y.M., Zhu, G.Q., 2015. FNDC5 overexpression and irisin ameliorate glucose/lipid metabolic derangements and enhance lipolysis in obesity. Biochim. Biophys. Acta 1852, 1867–1875.
Yan, B., Shi, X., Zhang, H., Pan, L., Ma, Z., Liu, S., Liu, Y., Li, X., Yang, S., Li, Z., 2014. Association of serum irisin with metabolic syndrome in obese Chinese adults. PLoS One 9, e94235.
Yang, Z., Chen, X., Chen, Y., Zhao, Q., 2015. Decreased irisin secretion contributes to muscle insulin resistance in high-fat diet mice. Int. J. Clin. Exp. Pathol. 8, 6490–6497.
Zhang, H.J., Zhang, X.F., Ma, Z.M., Pan, L.L., Chen, Z., Han, H.W., Han, C.K., Zhuang, X.J., Lu, Y., Li, X.J., Yang, S.Y., Li, X.Y., 2013. Irisin is inversely associated with intrahepatic triglyceride contents in obese adults. J. Hepatol. 59, 557–562.
Zhang, W., Chang, L., Zhang, C., Zhang, R., Li, Z., Chai, B., Li, J., Chen, E., Mulholland, M., 2015. Central and peripheral irisin differentially regulate blood pressure. Cardiovasc. Drugs Ther. 29, 121–127.
Zhang, Y., Li, R., Meng, Y., Li, S., Donelan, W., Zhao, Y., Qi, L., Zhang, M., Wang, X., Cui, T., Yang, L.J., Tang, D., 2014. Irisin stimulates browning of white adipocytes through mitogen-activated protein kinase p38 MAP kinase and ERK MAP kinase signaling. Diabetes 63, 514–525.
Zhu, D., Wang, H., Zhang, J., Zhang, X., Xin, C., Zhang, F., Lee, Y., Zhang, L., Lian, K., Yan, W., Ma, X., Liu, Y., Tao, L., 2015. Irisin improves endothelial function in type 2 diabetes through reducing oxidative/nitrative stresses. J. Mol. Cell. Cardiol. 87, 138–147.